THE ASTRONOMICAL JOURNAL, 121:489–502, 2001 January

A SEARCH FOR L DWARF BINARY SYSTEMS

I. NEILL REID,[1] JOHN E. GIZIS,[2] J. DAVY KIRKPATRICK,[2] AND D. W. KOERNER[1]

Received 2000 July 11; accepted 2000 September 26

ABSTRACT

We present analysis of *Hubble Space Telescope* (*HST*) planetary camera images of 20 L dwarfs identified in the course of the Two Micron All Sky Survey. Four of the targets, 2MASSW J0746425+200032, 2MASSs J0850359+105716, 2MASSW J0920122+351742, and 2MASSW J1146345+223053, have faint red companions at separations between 0.″07 and 0.″29 (1.6–7.6 AU). Ground-based infrared imaging confirms the last as a common proper motion companion. The surface density of background sources with comparable colors is extremely low, and we identify all four as physical binaries. In three cases, the bolometric magnitudes of the components differ by less than 0.3 mag. Since the cooling rate for brown dwarfs is a strong function of mass, similarity in luminosities implies comparable masses. The faint component in the 2M0850 system, however, is over 1.3 mag fainter than the primary in the I band and $\sim$0.8 mag fainter in $M_{\rm bol}$. Indeed, 2M0850B is $\sim$0.8 mag fainter in I than the lowest luminosity L dwarf currently known, while the absolute magnitude we deduce at J is almost identical with M_J for Gl 229B. We discuss the implications of these results for the temperature scale in the L/T transition region. 2M0850 is known to exhibit 6708 Å Li I absorption, indicating that the primary has a mass less than 0.06 $M_\odot$. Theoretical models predict that the magnitude difference implies a mass ratio of $\approx$0.75. The apparent binary fraction of the current sample, 20%, is comparable to the results of previous surveys of late-type M dwarfs in the field and in the Hyades. However, the mean separation of the L dwarf binaries in the current sample is smaller than the M dwarf value by a factor of 2, and only one system would be detected at the distance of the Hyades. We discuss the likely binary frequency among L dwarfs in light of these new data.

Key words: binaries: general — stars: low-mass, brown dwarfs

1. INTRODUCTION

The hypothesis that stars might form gravitationally bound binary systems dates to 1783 with John Goodricke's explanation of the periodic luminosity variations in both β Persei (Algol) and δ Cephei. Subsequent observations (reported by Pickering in 1881) confirmed at least the former case, and the frequency of binarity as a function of spectral type is now recognized as a significant constraint on global star formation theories. Moreover, binarity may influence the characteristics of planetary systems by affecting the structure and extent of protoplanetary disks.

The frequency of stellar-mass companions varies with the mass of the primary. The multiple star fraction (MSF) is defined as the fraction of stellar systems that are binary or multiple. Studies of solar-type stars (Duquennoy & Mayor 1991) indicate a high MSF, exceeding 60%. In contrast, surveys of lower mass M dwarfs find a multiplicity frequency of 35%, with companions at separations from 0.01 to 2500 AU (Fischer & Marcy 1992; Reid & Gizis 1997a, 1997b). Approximately 5% of M dwarfs in the solar neighborhood are companions of more massive stars (spectral type K and earlier). Overall, 60% of M dwarf systems are single.

In contrast, recent observations have resulted in the identification of a surprisingly large number of binaries among the lower temperature, lower mass L dwarfs discovered in the course of the new generation of near-infrared sky surveys. Two of the three L dwarfs in the original DENIS brown dwarf minisurvey (Delfosse et al. 1997) prove to be binary (Martín, Brandner, & Basri 1999; Koerner et al. 1999, hereafter Ko99). Three of 10 L dwarfs observed by Ko99 using the Near-Infrared Camera (NIRC) on Keck are identified as binaries.

At first sight, these results suggest a high binary fraction for L dwarf systems. However, almost all of the binaries detected to date are spatially resolved systems with equal-luminosity components at separations of $<$0.″5, unresolved in the original infrared surveys. Both the DENIS (Delfosse et al. 1997) and 2MASS (Kirkpatrick et al. 1999b, 2000a; hereafter K99 and K00, respectively) L dwarf samples are drawn from magnitude-limited catalogs. As pointed out by Öpik (1924) and Branch (1976), the larger effective sampling volume leads to enhanced numbers of equal-luminosity binaries under such circumstances.

We are currently undertaking a project that aims at a definitive measurement of the binary frequency among ultracool dwarfs (spectral types $\geq$M8) by combining high-resolution imaging with the planetary camera of the *Hubble Space Telescope* (*HST*) and high-resolution spectroscopy with NIRSPEC on Keck. This paper presents the first results from this program: *HST* images of 20 L dwarfs, four of which are resolved as binaries. Unlike most previous discoveries, one of the systems discussed in this paper has a secondary component significantly fainter than the system primary. That system, therefore, has a mass ratio, M_2/M_1 (or q), less than unity. The following section presents the observations, and the final section discusses the implications of these results.

[1] Department of Physics and Astronomy, University of Pennsylvania, 209 South 33d Street, Philadelphia, PA 19104-6396; inr@morales.physics.upenn.edu.

[2] Infrared Processing and Analysis Center, MS 100-22, California Institute of Technology, Pasadena, CA 91125; davy@ipac.caltech.edu, gizis@ipac.caltech.edu.

2. OBSERVATIONS

Table 1 lists the L dwarfs targeted for observation. All were identified based on their extremely red near-infrared colors ($J-K_S > 1.3$ mag) measured in the 2MASS survey, and each has been confirmed as spectral type L based on follow-up spectroscopy. Optical spectra of 2M0850, 2M0913, 2M1146, 2M1155, 2M1328, 2M1439, and 2M1632 (we adopt this abbreviated nomenclature for each source) are presented by K99; observations of 2M0036, 2M0746, and 2M1507 are discussed by Reid et al. (2000); and the remaining L dwarfs are included in K00. Four of the targets have lithium absorption: 2M0825, 2M0850, 2M1146, and 2M1726 have features with equivalent widths of 10, 15, 5, and 6 Å, respectively, indicating masses below 0.06 $M_\odot$ (Rebolo, Martín, & Magazzu 1992). The available spectroscopic observations allow us to set upper limits of 1 Å on λLi 6708 for 14 of the 16 remaining dwarfs; low signal-to-noise data for 2M0708 and 2M1623 lead to upper limits of only 5 Å. All are likely to have masses close to or below the hydrogen-burning limit.

Each L dwarf was imaged on the planetary camera (PC) chip of WFPC2, using both F814W and F606W filters. The camera has a plate scale of 0.″0455 pixel^{-1}, and the F814W (I band) exposure times were adjusted to provide the maximum dynamic range for companion detection without saturating the target. Table 2 gives the journal of observations. The analysis techniques used are discussed in Reid & Gizis (1997a, 1997b). In brief, our observations are capable of detecting equal-luminosity binaries with separations, Δ, of more than 0.″09, with limiting sensitivities of $\Delta I_{B-A} = 1$, 3, and 5 mag at $\Delta = 0.''14$, 0.″23, and 0.″31, respectively, where ΔI_{B-A} is the magnitude difference between secondary and primary. The maximum radius for companion detection, 18.″2, is set by the angular field of view of the PC chip. The 2MASS scans allow us to search for L and T dwarf companions brighter than $J = 16$ at wider separations. At the average distance of the present sample, 20 pc, equal-luminosity binaries are detectable at separations between 1.8 and 360 AU.

Accurate positions for each source (from 2MASS) are given in Table 1, where we also list spectral types, parallax estimates, and both I-band and infrared photometry. The trigonometric parallax measurements are from USNO observations (Dahn et al. 1999), updated in a few cases to include more recent observations (C. Dahn 1999, private communication). Only nine L dwarfs including three binaries have ground-based I_C photometry from USNO observations (Dahn et al. 1999). However, we have used DAOPHOT to measure I_{814} magnitudes for all of the sources, adopting the zero point derived in the Holtzman et al. (1995) calibration. Clearly, all of our targets are significantly redder than any of the calibrating stars observed by Holtzman et al., and we have used the six apparently single dwarfs in this sample to determine the extent of any color term. Figure 1 shows the results. The available data can be represented by a linear correction

$$\delta I = I_C - I_{814} = -(0.534 \pm 0.439) + (0.230 \pm 0.121)(I_{814} - J) .$$

Neither the slope nor the zero point of the fit is strongly constrained. However, the dispersion about the relation is only 0.06 mag, and eliminating the single most discrepant point (at $\delta I = 0.44$ mag) gives

$$\delta I = I_C - I_{814} = -(0.285 \pm 0.271) + (0.155 \pm 0.076)(I_{814} - J) ,$$

reducing δI by only 0.05 mag at $(I_{814}-J) = 4$. These uncertainties are not important in the present context. The

TABLE 1

ASTROMETRIC AND PHOTOMETRIC DATA

2MASS	Sp.	Ref.	π (mas)	M_I	$I-J$	M_J	$J-K$
W J0036159+182110.....	L3.5	R00	112.4 ± 2.0[a]	16.36 ± 0.05[c]	3.67	12.69[c]	1.38 ± 0.03
W J0708213+295035.....	L5	K00	23 ± 3.5[b]	17.51 ± 0.35[d]	3.98	13.53	2.06 ± 0.15
W J0740096+321203.....	L4.5	K00	27 ± 4[b]	17.07 ± 0.35[d]	3.74	13.33	1.99 ± 0.11
W J0746425+200032.....	L0.5	R00	83 ± 2[a]	14.69 ± 0.06[c]	3.38	11.31[c]	1.24 ± 0.04
W J0820299+450031.....	L5	K00	28 ± 4[b]	17.65 ± 0.35[d]	4.13	13.52	2.06 ± 0.14
W J0825196+211552.....	L7.5	K00	80 ± 12[a]	18.29 ± 0.30[e]	4.23	14.06[c]	1.97 ± 0.10
s J0850359+105716	L6	K99	36.1 ± 4.4[a]	18.21 ± 0.25[c]	4.31	13.90[c]	1.85 ± 0.06
W J0913032+184150.....	L3	K99	29 ± 4[b]	16.83 ± 0.35[d]	3.63	13.20	1.72 ± 0.09
W J0920122+351742.....	L6.5	K00	48 ± 7[b]	17.68 ± 0.35[d]	3.73	13.95	1.66 ± 0.11
W J0928397−160312.....	L2	K00	26 ± 4[b]	15.96 ± 0.35[d]	3.55	12.41	1.70 ± 0.07
W J1123556+412228.....	L2.5	K00	20 ± 3.5[b]	16.32 ± 0.35[d]	3.75	12.57	1.70 ± 0.07
W J1146345+223053.....	L3	K99	38.2 ± 1.3[a]	15.76 ± 0.05[c]	3.73	12.03[c]	1.53 ± 0.04
W J1155009+230706.....	L4	K99	30 ± 4.5[b]	17.12 ± 0.35[d]	3.73	13.39	1.68 ± 0.15
W J1328550+211449.....	L5	K99	26.3 ± 4.9[a]	17.19 ± 0.35[c]	4.12	13.07[c]	1.85 ± 0.05
W J1338261+414034.....	L2.5	K00	44 ± 7[b]	15.89 ± 0.35[d]	3.45	12.44	1.47 ± 0.05
W J1343167+394508.....	L5	K00	29 ± 4[b]	17.47 ± 0.35[d]	3.98	13.49	2.07 ± 0.10
W J1439284+192915.....	L1	K99	69.8 ± 0.6[a]	15.34 ± 0.18[c]	3.43	11.91[c]	1.20 ± 0.03
W J1507476−162738.....	L5	R00	131.0 ± 23.2[a]	17.24 ± 0.35[c]	3.83	13.41[c]	1.42 ± 0.03
W J1632291+190441.....	L8	K99	59.5 ± 2.9[a]	18.86 ± 0.11[c]	4.18	14.68[c]	1.86 ± 0.05
W J1726000+153819.....	L2	K00	50 ± 7.5[b]	18.05 ± 0.35[d]	3.91	14.14[d]	2.01 ± 0.08

[a] USNO trigonometric parallax (Dahn et al. 1999).
[b] Photometric parallax estimate (K99/K00).
[c] I_C, J, and K photometry from USNO observations (Dahn et al. 1999).
[d] I_C computed from I_{814} using the relation given in § 2.
[e] I_C from C. Dahn 1999, private communication.

REFERENCES.—(K99) Kirkpatrick et al. 1999b; (K00) Kirkpatrick et al. 2000a; (R00) Reid et al. 2000.

TABLE 2

JOURNAL OF OBSERVATIONS

Source	Epoch	F606W Exposure (s)	F814W Exposure (s)	l (deg)	b (deg)	N_b [a]
2M0036.....	2000 Feb 15	100	3 × 100	119	−44	2
2M0708.....	2000 Mar 23	100	300, 350	188	17	10
2M0740.....	2000 Mar 27	110	300, 350	188	25	14
2M0746.....	2000 Apr 15	50	3 × 50	201	21	5
2M0820.....	2000 Apr 24	100	300, 350	175	35	7
2M0825.....	2000 Mar 25	100	300, 350	203	30	10
2M0850.....	2000 Feb 1	100	300, 350	209	32	3
2M0913.....	2000 Apr 5	100	300, 350	211	40	5
2M0920.....	2000 Feb 9	100	300, 350	189	45	16
2M0928.....	2000 Apr 28	100	300, 350	249	25	3
2M1123.....	2000 Apr 19	100	300, 350	169	68	5
2M1146.....	2000 Apr 28	100	300, 350	228	75	6
2M1155.....	2000 Mar 18	100	300, 350	229	77	8
2M1328.....	2000 Apr 23	100	300, 350	0	79	4
2M1338.....	2000 Apr 25	100	300, 350	91	73	3
2M1343.....	2000 Apr 21	100	300, 350	84	73	5
2M1439.....	2000 Mar 22	100	3 × 100	21	63	5
2M1507.....	2000 Feb 24	100	3 × 140	89	34	7
2M1632.....	2000 Apr 20	100	300, 350	36	39	6
2M1726.....	2000 Mar 24	100	300, 350	28	25	14

[a] N_b is the number of stellar sources in each PC frame with $I_{814} > 20.5$ mag.

increase in δI at later spectral types probably reflects the steep spectral slope at <9000 Å due to broad K I λ7665/7699 absorption. We have used the steeper relation to transform the WFPC2 I_{814} magnitudes to the Cousins I-band (hereafter, we use M_I to denote absolute magnitudes on the Cousins system, and M_{814} for the *HST* system). Figure 2 plots the location of our targets on the (M_J, I_C-J) plane.

The linear color term we derived above is unlikely to be valid at redder colors. Gl 229B is the only T dwarf with *HST* photometry. Golimowski et al. (1998) measure $M_{814} = 20.76$, giving an $I_{814}-J$ color of 5.26 mag (adopting the J-band magnitude measured by Leggett et al. 1999) and predicting $\delta I = 0.68$ mag. Matthews et al. (1996) list the absolute magnitude as $M_i = 21.2$. While this mea-

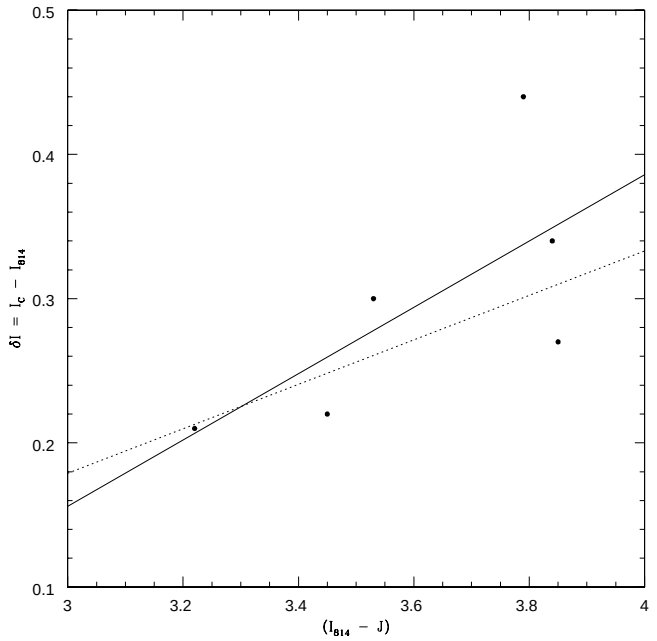

FIG. 1.—Offset between I_C and I_{814} as a function of $I_{814}-J$ color for L dwarfs. The solid line plots the best-fit linear relation, and the dashed line plots the linear regression if the most discrepant point is omitted from the sample.

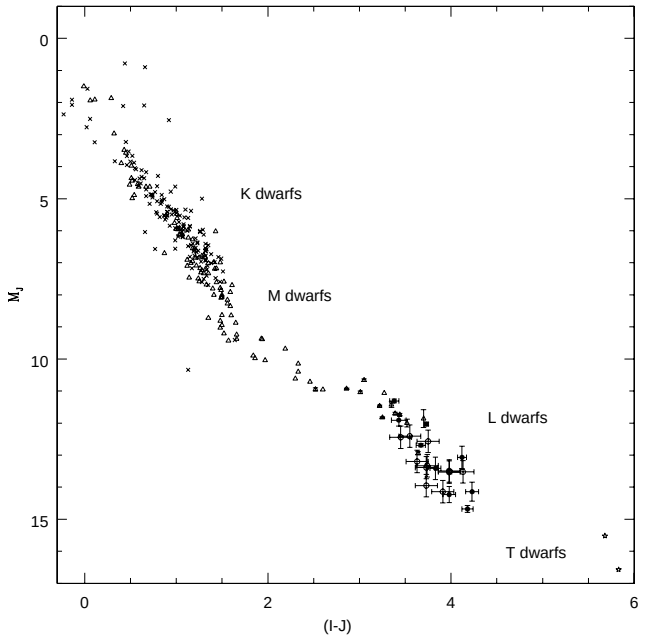

FIG. 2.—(M_J, I_C-J) diagram for low-mass dwarfs. Crosses are nearby stars with *BVRI* data from Bessell (1991), *JHK* observations from 2MASS, and parallax measurements from *Hipparcos*. Open triangles mark nearby, single stars with accurate trigonometric parallax measurements (from Reid & Gizis 1997b) and late M/L dwarfs from the USNO parallax program (Dahn et al. 2001). Solid points identify the nine L dwarfs in the present *HST* sample that have trigonometric parallax measurements (Dahn et al. 2001). The remaining 11 *HST* L dwarfs with spectroscopic parallax estimates are plotted as open circles. Finally, five-pointed stars mark data for the T dwarfs Gl 229B (Nakajima et al. 1995) and Gl 570D (Burgasser et al. 2000a).

surement was made with a Gunn i filter, the magnitude is tied to the Cousins flux zero point rather than to the AB magnitude system. Hence, the corresponding color is $(I_C - J) = 5.68$, equivalent to $\delta I \sim 0.42$ mag.

Sixteen of the 20 targets in the present sample show no evidence for duplicity in our observations; four dwarfs, however, have apparent companions at small angular separations (Figs. 3–6). Ground-based, near-infrared imaging had already identified 2M1146 as a likely binary source (Ko99). Our *HST* imaging confirms that observation, and using DAOPHOT we measure a separation of 0.″29 at a position angle of 199.°5 and a magnitude difference of $\Delta I_{814} = I_{814}(B) - I_{814}(A) = 0.31$ mag. This compares with $\Delta = 0.''29$, $\theta = 206°$, and $\Delta K = 0.1$ mag derived from NIRC observations (Ko99).

Reid et al. (2000) suggested 2M0746 as a binary candidate based on its location in the $(M_J, I-J)$ color-magnitude diagram, 0.7 mag brighter than the "main sequence." This suggestion proves to have merit, with the two components having $\Delta I_{814} = 0.62$ mag and a separation of 0.″22. 2M0920 is barely resolved but is clearly extended in the F814W image. Fitting the image profile using our 2M0036 observation as a point-spread function template, we derive $\Delta I_{814} = 0.4$ mag and $\Delta = 0.''07$.

The fourth binary candidate, 2M0850, is notable in that the resolved companion lying at a separation of 0.″16 is

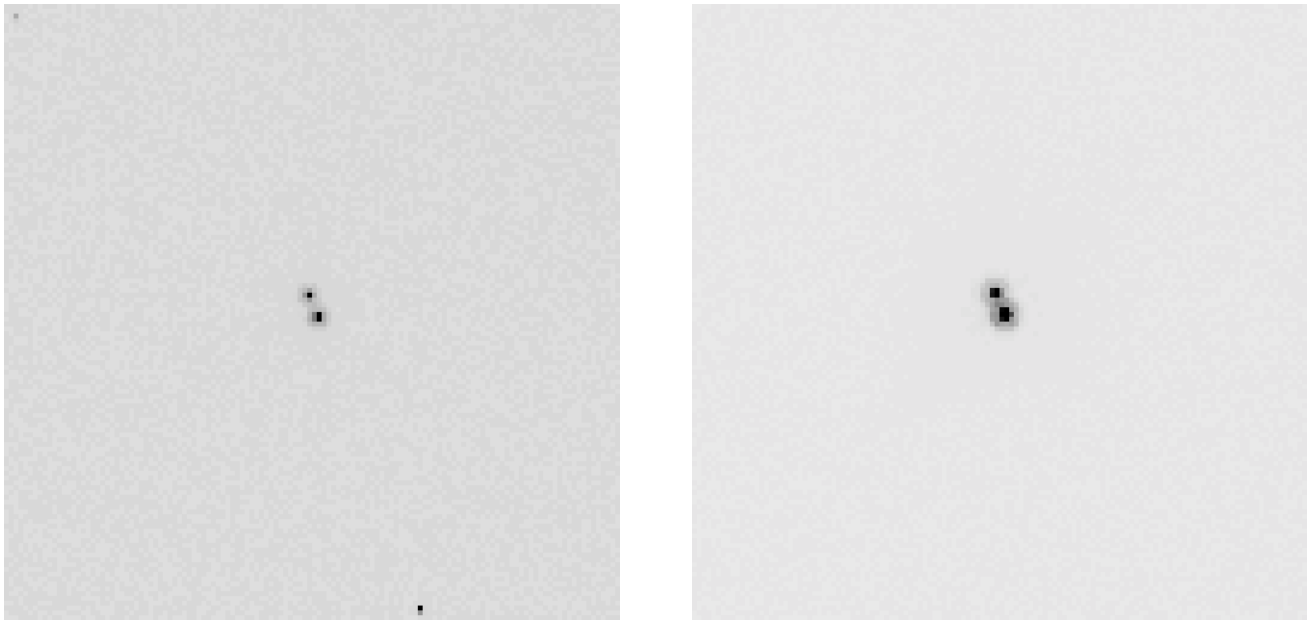

FIG. 3.—*HST* planetary camera images of 2M0746. The left panel shows the F606W exposure, the right panel shows the F814W image. The field of view is 6″ × 6″.

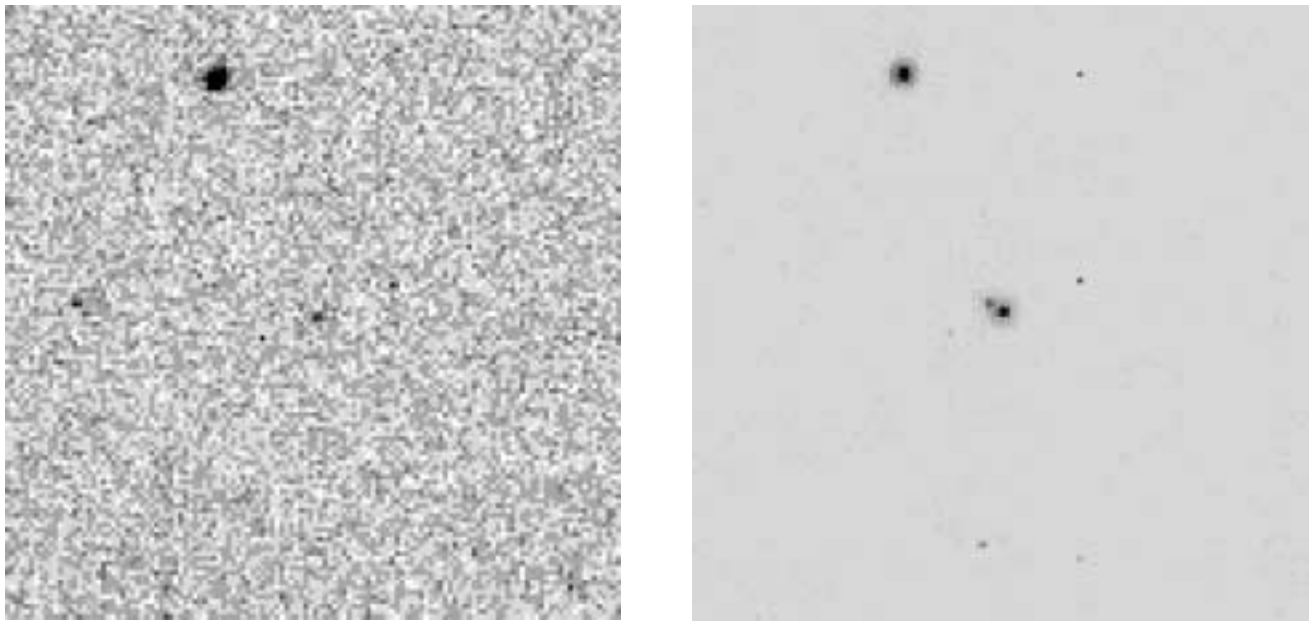

FIG. 4.—Same as Fig. 3 except for 2M0850. The bright object in the top left corner is an unrelated M dwarf.

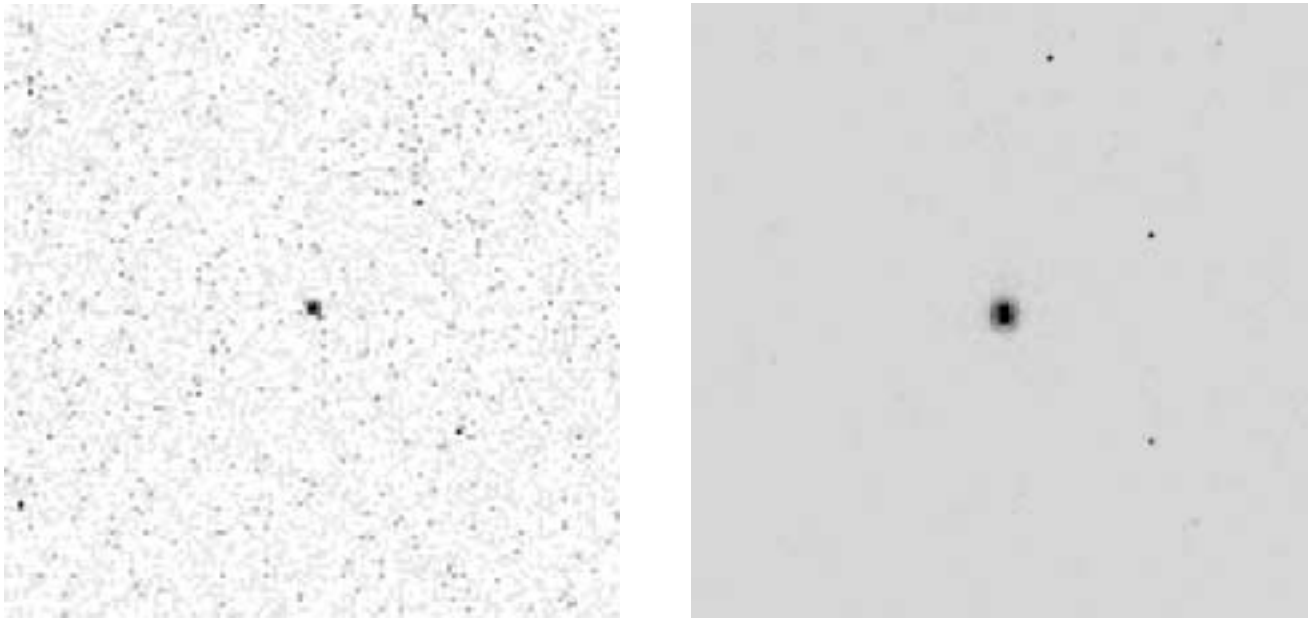

FIG. 5.—Same as Fig. 3 except for 2M0920

significantly fainter than the primary. We measure a relative magnitude of $\Delta I_{814} = 1.27$ mag. The individual magnitudes, based on the Holtzman et al. (1995) calibration, are $I_{814} = 20.44$ and 21.76 mag, and the fainter source is not detected in the F606W observation.

Are these apparent companions physically associated with the L dwarf targets? As Table 2 shows, all four candidate binaries lie at moderate to high Galactic latitude, with a correspondingly low surface density of background stars. There is no evidence that any of the companions are spatially extended as might be expected for background galaxies, although limits are less stringent for 2M0920. We have used standard filtering techniques to remove cosmic rays from the images, and Table 2 lists the number of faint ($I_{814} < 20.5$), stellar sources in each PC frame. The average surface density is 6.5 ± 3.6 sources per PC frame, implying an a priori probability of $\sim 3 \times 10^{-4}$ of finding a source within 0.″16 of a given point on the frame. Even in the more crowded field of 2M0920, the probability of association, given a random distribution of background sources, is only 4×10^{-3}.

Coincidence arguments are vulnerable to small number statistics. Faint background sources are, however, expected to be either K-type Galactic stars or low-redshift ($z < 0.5$) galaxies with similar colors, and all of the background sources we detect have neutral $R_{606} - I_{814}$ colors. In contrast, all of the potential companions have $R - I$ colors similar to the known L dwarf primaries, significantly redder than either K-type stars or galaxies. As a final test, Koerner & Kirkpatrick have deep near-infrared images ($K < 22$

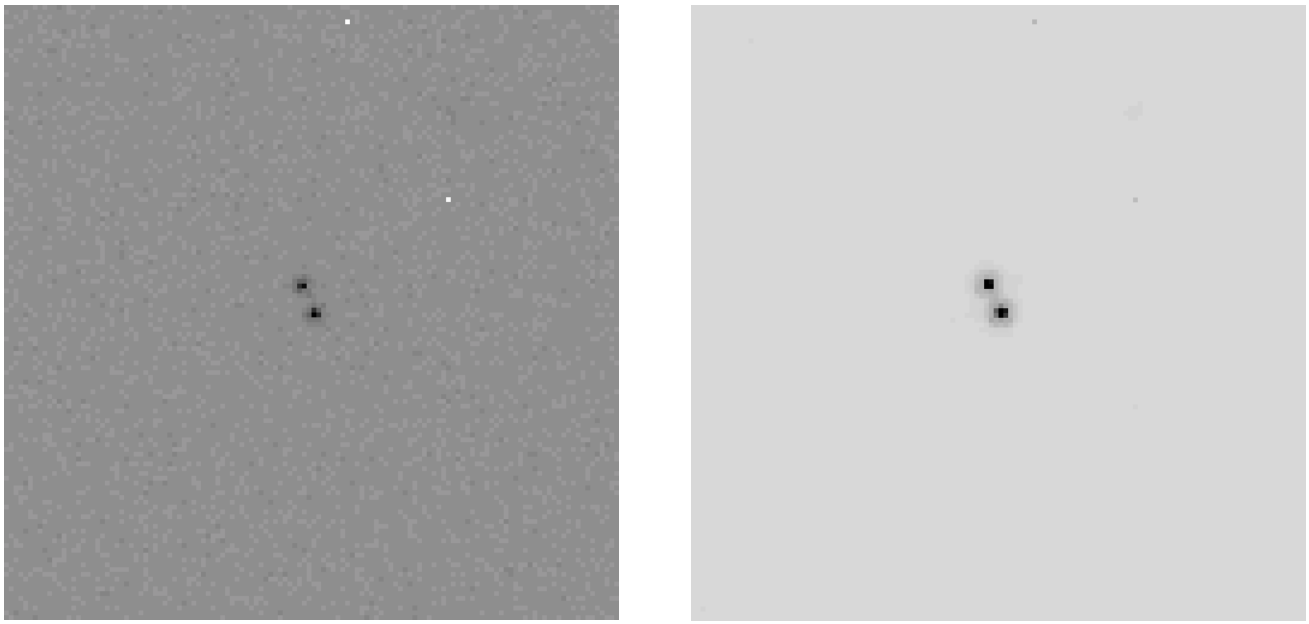

FIG. 6.—Same as Fig. 3 except for 2M1146

mag) of all four sources, obtained with the Keck Telescope one to two years before the *HST* observations. 2M1146A/B is confirmed as a common proper motion pair. The motions of 2M0746 and 2M0850 (0.″38 and 0.″16 yr^{-1}, respectively; Dahn et al. 1999) are sufficient that the companions should be resolved if either were a stationary background source: no such object is visible in either set of NIRC images. Thus, the preponderance of the evidence indicates that all four faint sources are physical companions of the respective L dwarf targets.

3. DISCUSSION

3.1. *Absolute Magnitudes and Luminosities*

Adopting the hypothesis that the sources are physically associated, Table 3 lists the absolute magnitudes derived for the individual components. We have used the relative fluxes measured from the WFPC2 F814W images to deconvolve the relative contribution of each star to the joint I-band photometry. We use a similar technique to estimate the individual J magnitudes. The L dwarf sequence has a slope of ~ 4 in the (M_I, $I_C - J$) color-magnitude plane (Fig. 7), and we estimate the relative magnitudes at 1.25 μm using

$$\Delta J \approx 0.75 \Delta I_C \, .$$

Absolute magnitudes for each component can then be derived from M_J(AB).

Figure 7 plots the location of each component in the (M_I, $I_C - J$) plane. The two most luminous systems, 2M0746 and 2M1146, are both overluminous in Figure 2, which plots the joint, ground-based photometry. Figure 7 shows that the individual components of both systems lie squarely within the L dwarf sequence.[3] These are two of the brightest L dwarfs known; indeed, 2M0746 is currently the brightest, with an apparent magnitude of $K = 10.49$. The fact that both prove to be binaries, as have two of the three bright L dwarfs discovered in the initial DENIS brown dwarf mini-survey (Delfosse et al. 1997), is a clear example of Öpik's equal-mass binary selection effect.

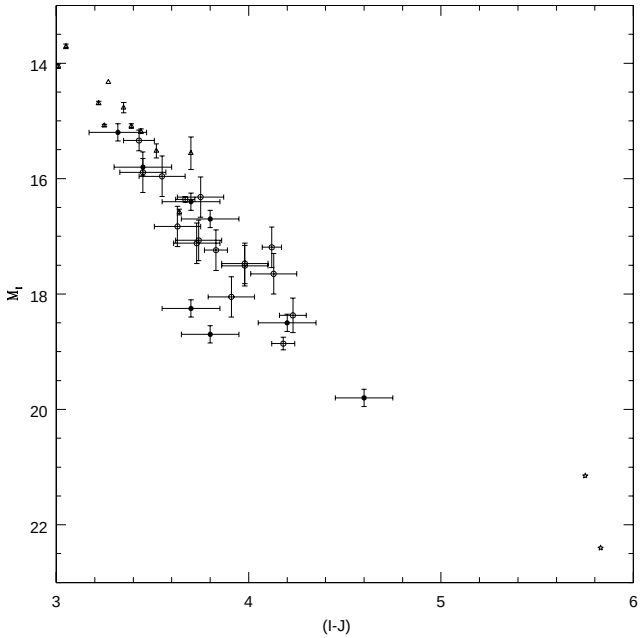

FIG. 7.—M_I, $I_C - J$ color-magnitude diagram for ultracool dwarfs. As in Fig. 2, open triangles mark data for nearby late-type M dwarfs and L dwarfs with trigonometric parallax measurements. The open circles plot data for the apparently single L dwarf with *HST* observations. Filled circles (*with error bars*) mark our estimates of the location of the four binary components.

Considering the two later type binaries, both components in 2M0920 lie 0.3 mag blueward of the L dwarf sequence. That system currently lacks a trigonometric parallax, and the absolute magnitudes are correspondingly less certain. Both components in 2M0850AB lie squarely on the sequence. There is something of a discrepancy between the observed spectral type, L6, and the absolute magnitude of 2M0850A, which is slightly fainter than the value derived for the L7.5 dwarf, 2M0825. This may simply reflect intrinsic scatter in the (M_I, spectral type) relation.

[3] Two unresolved systems are noticeably overluminous in Figure 7: PC0025, at $M_I = 15.5$, $(I_C - J) = 3.7$; and 2M1328, at $M_I = 17.2$, $(I_C - J) = 4.1$. Burgasser et al. (2000b) suggest that the former is an interacting red dwarf/brown dwarf binary. Both would repay further study.

TABLE 3

BINARY PARAMETERS

Source	Δ[a]	P.A. (deg)	M_I	BC_I	M^I_{bol}	M_J	M^J_{bol}	$\langle M_{bol} \rangle$	$\log(L/L_\odot)$
2M0746:									
AB.....	0.22	15	14.67	...	...	11.31	...	...	...
A	2.7	...	15.17	1.5	13.7	11.85	13.75	13.75	-3.6 ± 0.1
B.....	...	...	15.79	1.8	14.0	12.32	14.2	14.1	-3.75 ± 0.1
2M0850:									
AB.....	0.16	250	18.21	...	...	13.90	...	...	...
A	4.4	...	18.50	2.4	16.1	14.3	16.2	16.15	-4.6 ± 0.1
B.....	...	...	19.84	3.0	16.8	15.2	17.1	16.95	-4.9 ± 0.1
2M0920:									
AB.....	0.07	90	17.68	...	...	13.95	...	...	...
A	1.6	...	18.26	2.3	15.95	14.55	16.45	16.2	-4.6 ± 0.1
B.....	...	...	18.70	2.6	16.1	14.9	16.8	16.35	-4.65 ± 0.1
2M1146:									
AB.....	0.29	199	15.76	...	...	12.03	...	...	...
A	7.6	...	16.37	1.8	14.6	12.67	14.6	14.6	-3.95 ± 0.1
B.....	...	...	16.68	2.0	14.7	12.90	14.8	14.75	-4.0 ± 0.1

[a] Units for AB are arcseconds, and for A astronomical units.

Given these observations, we have attempted the derivation of the luminosities of these systems. In principle, theoretical models can be used for this purpose. However, the flux distribution of ultracool dwarfs is affected by atmospheric dust, which starts to form at approximately spectral type M6. The emergent energy distribution predicted by stellar models is dependent strongly on the assumption made concerning the distribution of that dust, as illustrated most dramatically by Chabrier et al. (2000): dust-free and dusty models differ by over 2 mag in $J-K_S$; bolometric corrections have correspondingly large uncertainties. These problems are particularly acute for L-type dwarfs. Under such circumstances, we prefer to rely on empirical measurements.

Even so, it is clear that there is room for improvement in the definition of empirical bolometric corrections for late-type dwarfs. Figure 8 illustrates the current state of knowledge, plotting the available J-band and I_C bolometric corrections. While we have reliable measurements for Gl 229B (from Leggett et al. 1999), the latest type L dwarf with a bolometric magnitude estimate is the L4 dwarf GD 165B (Jones et al. 1994; Kirkpatrick et al. 1999a). Figure 8 plots those data, together with absolute magnitudes and bolometric corrections for the L2 dwarf, Kelu 1 (Ruiz, Leggett, & Allard 1997), and the M9.5 dwarf, BRI0021-0021 (Tinney, Reid, & Mould 1993). The arrows in the top panel for Figure 8 mark the observed locations of 2M0850A and 2M0850B.

We estimate M_{bol} for the binary components using two techniques. First, we use linear interpolation in the (M_I, BC_I) diagram. This approach may overestimate BC_I (M_{bol} too bright) in later type L dwarfs, since the bolometric correction must depend strongly on the extent of K I absorption, which is unlikely to increase in such a simple manner from L4 to T. Second, we combine the M_J values listed in Table 3 with an estimated $BC_J = 1.9$ mag (*bottom panel*, Fig. 8). Averaging those estimates, which generally agree to within 0.3 mag, gives the values of $\langle M_{bol} \rangle$ listed in Table 3. Luminosities are calculated for an adopted value of $M_{bol\odot} = 4.72$.

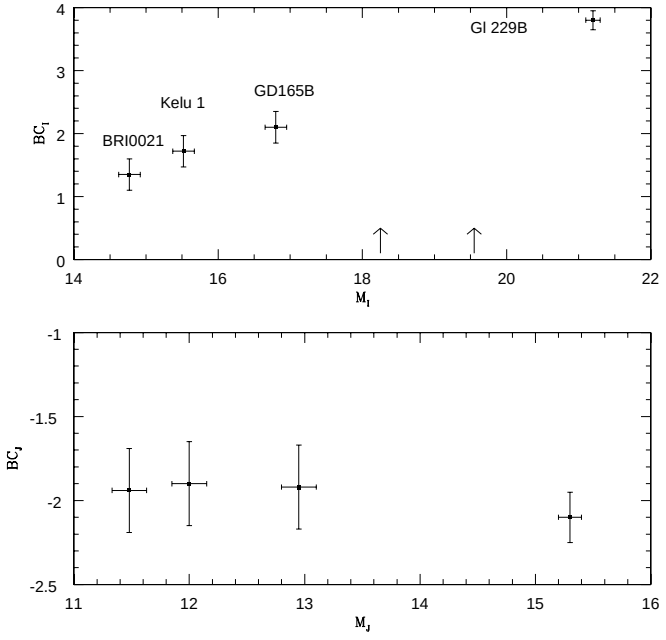

FIG. 8.—Bolometric corrections for late-type dwarfs. The top panel plots the available data for the Cousins I band, where the arrows mark the locations of 2M0850A and 2M0850B. The bottom panel plots (M_J, BC_J) data for the same four calibrators.

2M0850B stands out as particularly intriguing object. The I-band absolute magnitude is $\sim$0.9 mag fainter than the L8 dwarf, 2M1632 (Table 1), while the estimated J-band absolute magnitude, $M_J \sim 15.2$, is 0.2 mag fainter than faintest L dwarf currently known, Gl 584C (K00), and only 0.3 mag brighter than the value measured for Gl 229B (Leggett et al. 1999). Given these absolute magnitudes, the companion could be either a late-type L dwarf, spectral type $\approx$L9, or an early-type T dwarf. We discuss this system in more detail in § 3.3.

3.2. *Masses and Temperatures*

Our *HST* observations provide direct measurement of the relative magnitudes of the components; transforming those data to estimates of effective temperature and mass is not straightforward. Brown dwarfs evolve rapidly in luminosity and temperature as a function of mass. The components of a binary system, however, can be assumed to be coeval. Hence, the difference in luminosity observed for 2M0850A/B must be interpreted as a difference in mass. This is in contrast to most other known L dwarf binaries, in which both components have near-equal luminosity and, hence, near-equal mass. L and T dwarfs are known as secondary components of main-sequence stars (e.g., Gl 229B, Nakajima et al. 1995; G196-3, Rebolo et al. 1998) but at much wider separations (30 to 4000 AU). 2M0850A/B provides direct evidence that unequal-mass brown dwarf binaries can form at separations of <10 AU.

Evolutionary tracks for brown dwarfs of different masses lie in close proximity in the H-R diagram, overlapping tracks for low-mass stars at higher luminosities. As a result, the mass-luminosity relation is not single-valued in this regime, and we cannot estimate reliable masses for individual objects without knowledge of their age. However, if we can determine the bolometric magnitude of each component in a brown dwarf binary, we can use models to estimate a mass ratio based on the relative luminosity.

Given the luminosity estimates in Table 3, we have used theoretical models computed by Burrows et al. (1993, 1997) to constrain the values of relative masses in the lower luminosity systems, 2M0920 and 2M0850. As noted above, the presence of lithium in the optical spectrum of 2M0850 sets an upper limit of 0.06 $M_\odot$ on the mass of the primary component in that system. Both components of 2M0920AB have luminosities similar to the value for 2M0850A, but spectroscopic observations set an upper limit of 0.5 Å for the equivalent width of the Li 6708 Å line. Theoretical models predict that lithium is removed from the gas phase as solid LiCl at low temperatures (Fegley & Lodders 1996; Burrows & Sharp 1999; Lodders 1999), and spectroscopy of L dwarfs indicates that the strength of Li λ6708, when detected, decreases among the latest spectral types (K00). However, $\sim$50% of L6/L6.5 dwarfs have detectable lithium, so it is more reasonable to assume that the absence of lithium in 2M0920 is due to destruction through fusion, rather than solidification. In that case, both components in 2M0920AB have masses exceeding 0.06 $M_\odot$.

Accepting these hypotheses, Figure 9 (*top*) superposes the luminosity estimated for each of the four binary components on the [log(L), log(age)] plane. Figure 9 (*bottom*)

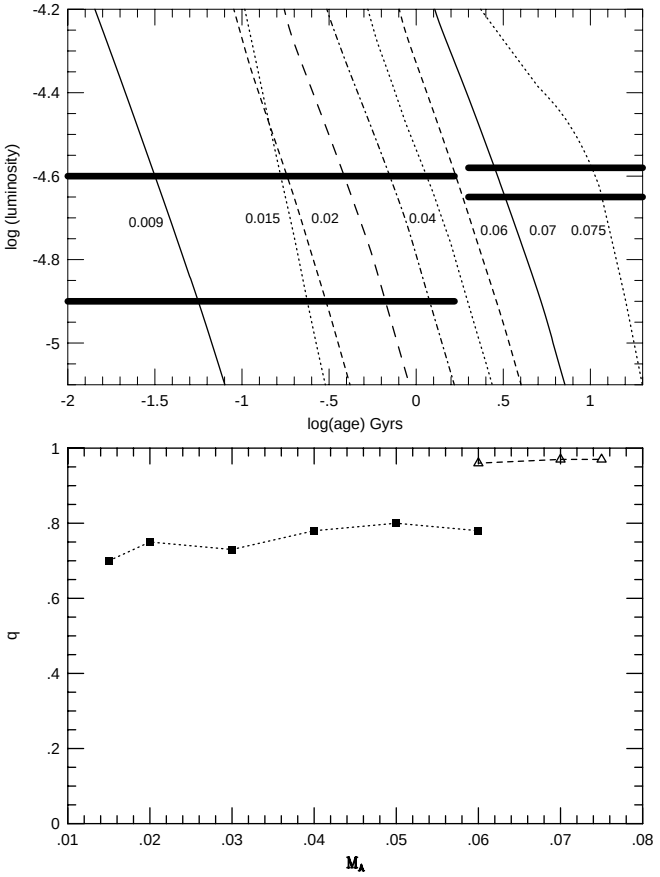

FIG. 9.—Mass estimates for 2M0850AB and 2M0920AB. The top panel plots evolutionary tracks for brown dwarfs calculated by Burrows et al. (1993, 1997). The solid horizontal lines plot the luminosity estimates for the four components. The left pair of lines plot 2M0850A and B, with the upper mass limit for 2M0850A set at 0.06 $M_\odot$ through the detections of lithium. The right-hand pair of lines, closer spaced in luminosity, mark 2M0920A and B. In the latter case, the nondetection of lithium sets a lower mass limit of 0.06 $M_\odot$ for 2M0920B. The bottom panel plots the inferred mass ratios for the two systems, with squares marking 2M0850A/B and triangles marking the near–equal–mass 2M0920A/B system.

plots the corresponding mass ratios, q. In both cases, the latter parameter varies over a relatively small range, with $q \sim 0.96$ for 2M0920AB and $q \sim 0.75$ for 2M0850AB. This sets an upper limit of 0.05 $M_\odot$ for the mass of 2M0850B.

The Burrows et al. (1993, 1997) models also allow us to estimate approximate temperatures for each component, given a particular value for the primary mass (i.e., age). Table 4 lists those values, where we have interpolated between tracks as necessary. We note that there are some inconsistencies, particularly at low masses and/or young ages. For example, if 2M0850A has $M \sim 0.02\ M_\odot$, Figure 9*a* implies $\tau \sim 0.19$ Gyrs and $\sim 0.015\ M_\odot$ for 2M0850B; a 0.015 $M_\odot$ brown dwarf is predicted to have a $\log(L/L_\odot) \sim -4.7$ at that age, however, rather than the observed $\log(L/L_\odot) \sim -4.9$. Nonetheless, these calculations provide a preliminary indication of the properties of the components in each system.

TABLE 4

MASS ESTIMATES (2M0850)

Age (Gyrs)	M_A ($M_\odot$)	M_B ($M_\odot$)	$T_{\rm eff}$ (A)	$T_{\rm eff}$ (B)
0.19.....	0.02	0.015	1210	1140
0.40.....	0.03	0.022	1260	1100
0.71.....	0.04	0.031	1310	1140
1.17.....	0.05	0.04	1350	1160
1.72.....	0.06	0.047	1380	1230

Figure 10 illustrates the results, superposing the error boxes on the theoretical H-R diagram for both components of 2M0850 and for 2M0920A. The similarity in spectral types between the composite spectra of the two systems suggests that 2M0850A lies near the upper limit of the estimated mass range. The most probable masses for the individual components are therefore: 2M0850A, $0.05 \pm 0.01\ M_\odot$; 2M0850B, $0.04 \pm 0.01\ M_\odot$; 2M0920A, $0.068 \pm 0.008\ M_\odot$; and 2M0920B, $0.068 \pm 0.008\ M_\odot$.

There are fewer constraints on the masses of the components in the two earlier type binaries. As with 2M0850, lithium absorption in 2M1146 indicates masses below 0.06 $M_\odot$ for both primary and secondary. 2M0746, in contrast, is lithium free, and if the system is older than ~ 1 Gyr, the Burrows et al. models predict that both components exceed the hydrogen-burning mass limit; at age 10 Gyrs, both have masses of 0.085 $M_\odot$.

Reliable masses require orbit determination. Such measurements should be possible over a reasonable timescale for at least two of the four systems discussed here. The average observed separation of components in a binary system is 80% of the semimajor axis. Applying that rule of thumb to our observations and taking the mass limits estimated above, 2M0850AB is likely to have an orbital period of 43 yr, while 2M0920AB may have a period as short as 8.5 yr. The latter system may be amenable to astrometry with the next generation of optical interferometers. 2M0746 may be accessible to more conventional imaging; with a lower mass limit of 0.12 $M_\odot$ (total mass), a semimajor axis of 3.5

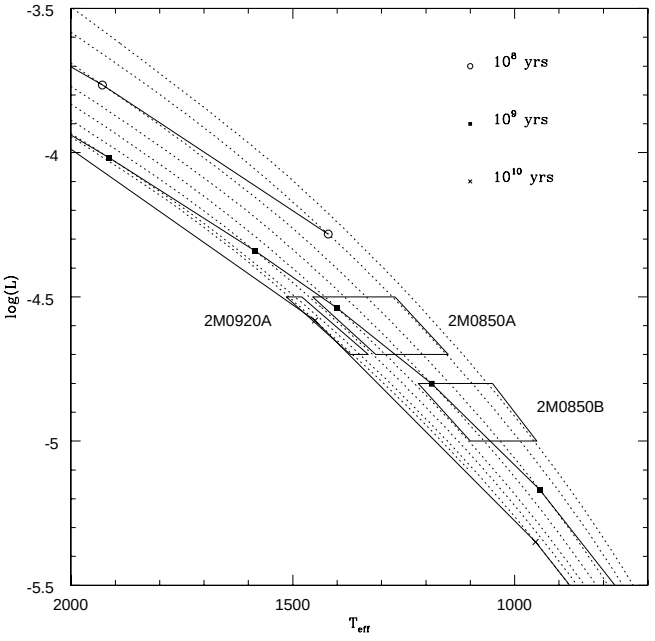

FIG. 10.—Error boxes for the brown dwarf components of 2M0850AB and for 2M0920A (2M0920B is not plotted) superposed on evolutionary tracks for brown dwarfs from Burrows et al. (1997). The solid lines mark 10^8, 10^9, and 10^{10} yr isochrones. The dotted lines mark the evolution of 0.015, 0.02, 0.03, 0.04, 0.05, 0.06, 0.07, and 0.075 $M_\odot$ models; the 0.015 $M_\odot$ model has the highest luminosity at a given temperature.

AU implies a period of less than 18 yr. In contrast, 2M1146 ($M_{tot} < 0.12\ M_\odot$) with $\langle a \rangle \sim 9.5$ AU has a likely period exceeding 85 yr.

3.3. *Temperature Scales, 2M0850, and the L/T Transition*

The extensive observational and theoretical work undertaken over the last few years has led to the emergence of a convincing qualitative scenario for brown dwarf spectral evolution. As the atmosphere cools below an effective temperature of $\sim$2500 K, first TiO and then VO solidify as dust particles, leaving metal hydrides as the strongest molecular features in the optical spectrum. The removal of these major opacity sources leads to increased atmospheric transparency, which, in turn, accounts for the presence of strong, pressure-broadened atomic lines of alkali metals (Na, K, Cs, Rb, Li). At near-infrared wavelengths, H_2O absorption dominates the spectrum, with CO as a prominent feature at 2.03 μm. As originally predicted by Tsuji (1964), carbon is bound preferentially in methane, rather than CO, at low temperatures, leading to strong absorption in the H and K windows, as in Gl 229B. This accounts for the blue near-infrared colors of T dwarfs, such as Gl 229B and Gl 570D.

The qualitative picture is clear. Quantitatively, however, we still lack a well-grounded temperature scale to associate with this behavior. The threshold temperature (if, indeed, there is a clean threshold) for the onset of methane absorption at 2 μm is important not only in understanding the structure of individual brown dwarfs but also in disentangling the underlying mass function from the observed number/spectral type surface densities (Reid et al. 1999). In broad terms, two temperature calibrations have been suggested. Basri et al. (2000) have combined model atmosphere calculations with high-resolution line profiles to derive temperatures of $\sim$2200 K for spectral type L0 and $\sim$1700 K for type L8 (K99 classification system). Noll et al. (2000) argue that the relatively weak 3.3 μm fundamental-band methane absorption detected in mid- and late-type L dwarfs favors this relatively hot scale, which implies a $\sim$700 K temperature difference between the latest L dwarfs and Gl 229B. If this temperature scale is correct, then there is a substantial population of early-type T dwarfs in the solar neighborhood, at least equal in number density to the known L dwarf population.

Photometric analyses, however, suggest lower temperatures. At least four currently known L8 dwarfs have values of M_J within 1 mag of Gl 229B ($M_J = 15.5$): 2M1632 ($M_J = 14.7$; Table 1), SDSSp J132629.82$-$003831.5 ($M_J = 14.8$; Fan et al. 2000), 2MASSW J0310599+164816 ($M_J = 14.9$; K00) and 2MASSW J1523226+301456 ($M_J = 15.0$; K00). The last mentioned dwarf is particularly important, since it is a proper-motion companion of the known nearby G dwarf binary, Gl 584AB, and therefore has a well-determined trigonometric parallax.

Late L and T dwarfs have radically different colors. L8 dwarfs have $(I-J) \approx 4.2$ and $(J-K) \approx 2$, as compared with $(I-J) \approx 5.7$ and $(J-K) \approx 0$ for Gl 229B. However, those differences are tied strongly to the relative strength of individual absorption features, broad K I at I and CH_4 overtone bands at H and K, rather than substantial variation in the underlying energy distribution. In contrast, the J band is largely free of significant absorption features. The crucial question is how well the flux in that passband tracks bolometric magnitude. Is F_J/F_{bol} approximately constant, as Figure 8 suggests? The scarcity of mid-infrared data for ultracool dwarfs means that we cannot answer this question directly at present; however, we can examine some of the consequent eventualities.

Gl 229B, the original T dwarf, has an effective temperature of 960 $\pm$ 70 K (Marley et al. 1996). Since brown dwarf radii are set by degeneracy, we know that 2M1523 (Gl 584C) and Gl 229B have radii that differ by, at most, 15%. We have

$$\frac{L_1}{L_2} = \left(\frac{R_1}{R_2}\right)^2 \left(\frac{T_1}{T_2}\right)^4 .$$

Suppose that Gl 584C is a high-mass brown dwarf, with a radius 15% smaller than that of Gl 229B. In that case, if Gl 584C has $T_{eff} = 1700$ K, then $L_{Gl\,584C} \sim 5.5 L_{Gl\,229B}$, or $M_{bol} = 15.5$, and the J-band bolometric correction is only -0.5 mag. On the other hand, if we assume that the bolometric corrections outlined in Figure 8 are reliable, then $L_{Gl\,584C} \sim 2 L_{Gl\,229B}$. In that case, assuming a 15% difference in radius, Gl 584C is predicted to have a temperature 30% higher than that observed for Gl 229B. That is, the photometric temperature estimate for spectral type L8 is 1250 $\pm$ 100 K (K00), $\sim$250 K cooler than Basri et al.'s spectroscopic estimate.

Figure 2 underlines visually the photometric hypothesis, which is essentially a continuity argument. The L dwarf sequence spans a 3 mag range in the J band, $12 \leq M_J \leq 15$; Basri et al. assign a corresponding temperature range of 500 K. Under this scenario, the 0.5 mag range $15 \leq M_J \leq 15.5$ between Gl 584C and Gl 229B corresponds to a temperature difference of 700 K. The corresponding photometric calibration assigns a temperature difference of $\sim$750 K (2000 to 1250 K) to the L dwarf sequence and $\sim$250 K to the latter interval.

The discovery by the SDSS collaboration of three field brown dwarfs with both CO and CH_4 absorption (Leggett et al. 2000) will clearly contribute valuable information on this problem. The coexistence of CO and methane in so many systems is surprising, since theoretical models predict their coexistence over a relatively narrow range in temperature (Fegley & Lodders 1996). This apparent paradox might be resolved through a combination of two factors: first, binarity (as discussed further below) and second, the nongray nature of late L/T dwarf atmospheres. As with Jupiter, topographical structures (bands, spots, zones) may allow us to see to different depths at different physical locations: that is, the overall energy distribution is produced by a range of temperatures, rather than being characterized by a single effective temperature, as is usually taken to be the case in hotter stellar atmospheres. For example, the 3.3 μm methane fundamental band is believed to be produced at higher levels in the atmosphere (lower pressure, lower temperature) than are responsible for the "continuum" flux in late L dwarfs. Under such inhomogeneous conditions, both CO and the overtone 1.6 and 2.1 μm CH_4 bands might be detectable in brown dwarfs spanning a broader range in luminosity than expected.

As yet, none of the SDSS T dwarfs has a known luminosity. 2M0850AB has a measured trigonometric parallax, allowing us to locate both components on the H-R diagram (Fig. 7). Thus, this system and others like it offer the prospect of providing valuable insight into this matter by linking the unknown (2M0850B) with the barely known (2M0850A).

The onset of detectable methane absorption in the K window defines the transition from spectral class L to class T (K99). Photometrically, however, we must make a distinction between cool dwarfs like Gl 229B, with near-saturated methane absorption in the H and K bands and A-type near-infrared colors, and the objects discovered recently by Leggett et al. The latter are by definition T dwarfs, since CH_4 is evident at K, but their near-infrared colors are closer to those of M giants, reflecting the weaker CH_4 absorption. We will refer to these objects as early-type T dwarfs and describe the more familiar Gl 229B–like objects as "classical" T dwarfs.

Given its absolute magnitude, 2M0850B might be a very late type L dwarf, an early-type T dwarf, or a "classical" T dwarf. High spatial resolution near-infrared photometry would allow us to discriminate among these options, since each occupies a distinct location in the $J-H/H-K$ plane. Currently, we lack such data, but the ground-based photometry listed in Table 1, together with K-band spectroscopy (K99), allow us to set limits on the nature of the companion. Based on the slope of the (M_I, $I-J$) L dwarf sequence, we inferred $\Delta J_{B-A} \sim 1$ mag, which implies that 2M0850B supplies $\sim 30\%$ of the flux at 1.25 μm in joint photometry. Late-type L dwarfs have similar $J-K$ colors, so one would expect a similar contribution at K in an L dwarf/L dwarf binary system. In contrast, Gl 229B loses $\sim 70\%$ of its K-band flux to methane absorption, so given the same ΔJ_{B-A}, an L dwarf/classical T dwarf system would be ~ 0.2 mag bluer in $J-K$ than an L dwarf/L dwarf binary. L dwarf/early T dwarf binaries will have intermediate $J-K$ colors.

2M0850AB has a $J-K$ color of 1.85 ± 0.06 mag. In comparison, 2M0825 and 2M1632, the two apparently single L dwarfs closest to 2M0850A in M_I, have $J-K$ colors of 1.97 ± 0.10 and 1.86 ± 0.05 mag, respectively. All three dwarfs have photometry from the same source (USNO), so this comparison indicates that 2M0850 is not unusually blue for its spectral type and absolute magnitude.

We have modeled the spectrum of a hypothetical late L/T dwarf binary by combining our CGS4 observations of the L7 dwarf, DENIS-P 0205.4-1159 (Reid et al. 2001), with similar data for Gl 229B (Geballe et al. 1996). Using IRAF, the data were binned to the same scale (5 Å pixel^{-1}) and summed, adopting $\Delta J_{B-A} = 1$ mag. The combined spectrum is plotted in Figure 11 and compared with our K-band data for 2M0850AB (K99). The J-band magnitude difference we infer for the components corresponds to $\Delta H_{B-A} \sim 2$ mag and $\Delta K_{B-A} \sim 2.6$ mag. However, the extensive methane absorption in a Gl 229B–like T dwarf leads to a significantly smaller flux difference in the shorter wavelength half of both H and K passbands, and the companion distorts the composite spectral energy distribution at those wavelengths, particularly in the H band.

Figure 11 shows that the 2M0850AB K-band observations are a reasonable match to our hypothetical composite spectrum at $\lambda > 2.15$ μm but fall below the predicted flux distribution at shorter wavelengths. A T dwarf companion with strong CH_4 absorption would be expected to make the most significant contribution in the latter spectral region. Thus, the observed discrepancy argues against that option.

There is a noticeable similarity between the near-infrared spectrum of our hypothetical late L/T dwarf binary and data for the early-type T dwarfs identified by Leggett et al.

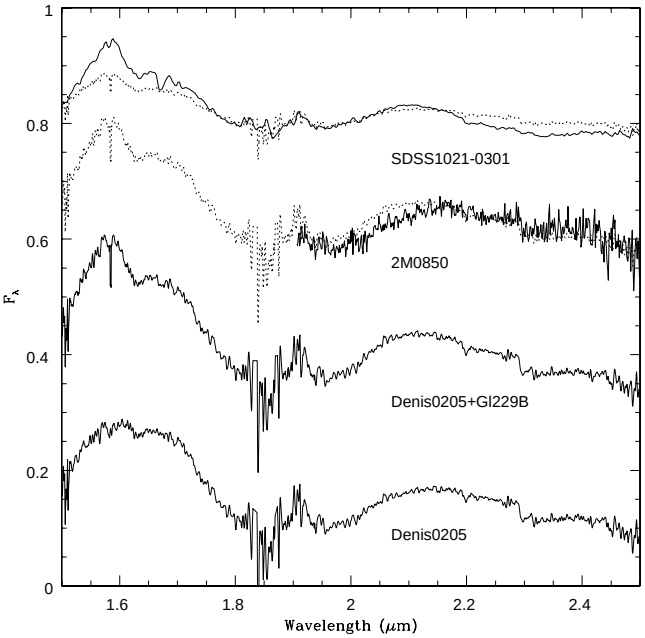

FIG. 11.—Composite 1.5–2.5 μm spectrum of a hypothetical late L/T dwarf binary. The lowest spectrum plots our CGS4 data for the L7 dwarf, DENIS-P 0205.4−1159. Next, we plot the hypothetical binary, combining the DENIS 0205 spectrum with data for Gl 229B (Geballe et al. 1996), with $\Delta J_{B\text{-}A} = 1$ mag. Third from the bottom, we plot K-band data for 2M0850. The top spectrum plots CGS4 data for the early T dwarf, SDSS 1021−0301 (data courtesy of S. Leggett). The dotted line superposed on the latter two spectra plots the L/T composite, scaled to match at 2.15 μm.

(2000). Indeed, following Öpik's binary selection criterion, one might expect the brighter "early T dwarfs" to include a number of unresolved near–equal-mass L/T binaries, with relatively small magnitude differences ΔJ_{B-A} and Δz_{B-A}. Distinguishing those objects from isolated early T dwarfs should be possible by examining the strength of the weaker methane absorption bands (for example, the $2\nu_2$ 1.67 μm feature) in both H and K bands. Broadband colors may also provide discrimination: combining a late-type L dwarf of $(J-K) \sim 1.9$, with a T dwarf companion, $\Delta J_{B-A} = 0.0$, $\Delta K_{B-A} = 1.9$, will produce a joint color of $(J-K) \sim 1.3$ mag. Bluer colors, such as those observed for three of the SDSS early-type T dwarfs, can only be produced if the companion T dwarf is *brighter* than the late-type L dwarf in the J passband. Given the relatively low opacities in the J passband and the extremely nongray flux distribution at these low temperatures, such circumstances cannot be excluded.

Summarizing the discussion, both broadband photometry and the observed K-band spectrum suggest that 2M0850B is unlikely to be a classical T dwarf, with full-blown CH_4 absorption. It remains possible that the companion is an early-type T dwarf. Near-infrared photometry or spectroscopy of the individual components (or perhaps joint spectroscopy at H) should provide a definitive answer to this issue.

4. L DWARFS IN BINARY SYSTEMS

The ultimate goal of our program is a determination of the frequency of binary and multiple L dwarf systems. With observations of only 20 targets, our current conclusions must be tentative. Moreover, the present observing list is far from the complete, volume-limited sample that is ideally suited to this type of investigation. However, our obser-

vations are not limited to the brightest known L dwarfs and are therefore less subject to Öpik's equal-mass binary selection effect. Bearing these caveats in mind, our initial results suggest that the frequency of wide binaries among L dwarfs is *lower* than that observed for M dwarf stars.

4.1. *The HST Sample*

Figure 12 compares the observed magnitude difference, ΔI_{814}, for the four binaries detected in this sample against the formal detection limits for *HST* planetary camera observations (Reid & Gizis 1997b). Those limits may be overly pessimistic: 2M0920 lies slightly below those formal limits, while 2M0850AB is easily detected, despite its proximity to the detection limit at that separation. At larger separations, the 2MASS data allow us to exclude any L dwarf companions with $J < 16$ (typically, $M_J < 14.5$, $M_I < 18$) and $\Delta < 10'$. It is clear that the detected systems occupy only a small fraction of the total parameter space available for the detection of potential companions.

The frequency of resolved binary L dwarfs in the present sample is 20% ± 11%. We can match this statistic against results from three other high-resolution imaging surveys: Reid & Gizis (1997b) obtained WFPC2 images of 53 late-type M dwarfs in the Hyades, identifying nine (17% ± 7%) confirmed binaries; similarly, WFPC2 observations of 41 field M dwarfs resolved eight (19.5% ± 7.5%) as binary or multiple systems (Reid & Gizis 1997a); finally, none of the 27 Pleiades very low mass (VLM) dwarfs surveyed by Martín et al. (2000) with the NICMOS 1 camera have resolved companions. The last sample includes targets with masses comparable with those expected for our field L dwarfs, while the Hyades and field M dwarfs have higher masses, with approximate limits of $0.1M_\odot < M < 0.3M_\odot$ and $0.2M_\odot < M < 0.5M_\odot$, respectively.

Each of these four samples has a different mean distance. We take this into account by transforming the results to the linear regime. Taking the sensitivity limits plotted in Figure 12 as a template, we calculate the limiting absolute magnitude for companion detection as a function of separation, Δ, in AU. Combining the results for each target allows us to estimate completeness limits for each sample; that is, the fraction of targets where we would expect to detect a companion with a given absolute magnitude at a given linear separation. Figure 13 plots those results, where we show the 50% and 100% detection limits together with the detected companions and the approximate absolute magnitude range of the targets.

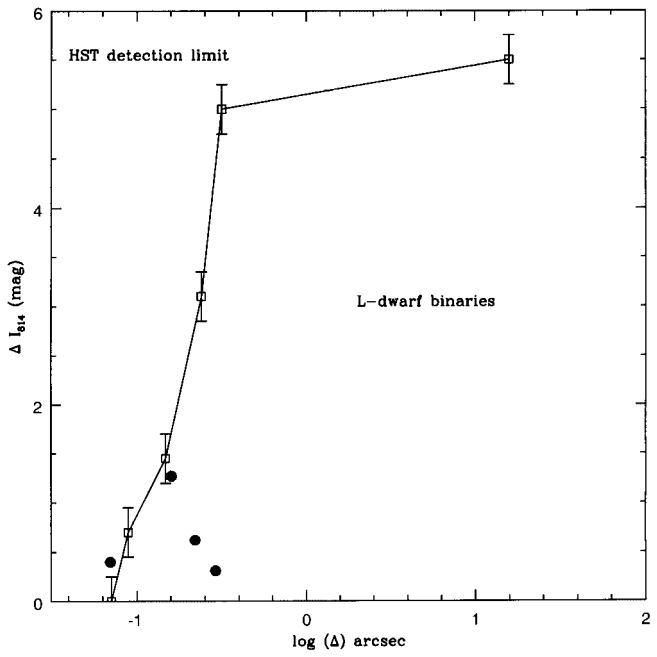

FIG. 12.—Comparison between the observed primary-secondary magnitude difference, ΔI_{F814}, and the formal detection limits of the *HST* planetary camera observations.

Simple visual comparison of the four panels in Figure 13 suggests a significant difference in the semimajor axis distribution of the M and L dwarf binaries: the L dwarf binaries all have separations of less than 10 AU, while the overwhelming majority of the M dwarf companions have $\Delta > 10$ AU. Indeed, were the L dwarfs to lie at the distance of the Hyades, we could expect to resolve only one system, 2M1146, while none would be resolved at the distance of the Pleiades. Martín et al. identify six Pleiades dwarfs (including PPl 15) as candidate photometric binaries. That fraction, 22% ± 9%, is consistent with the statistics of our L dwarf sample, where we resolve four systems and identify 2M1328 as a candidate photometric binary.

Conversely, the wider binaries present in the M dwarf samples are not present either in our L dwarf sample or, as already noted by Martín et al. (2000), among the Pleiades VLM dwarfs. Fourteen percent of the Hyades and field M dwarfs have companions at separations between 10 and 100 AU, with a further 5% having companions in the range 100 AU $< \Delta <$ 1000 AU. A similar distribution pertains for stars in the immediate solar neighborhood, with binary fractions of 5% at $\Delta \leq 1$ AU, 18% at 1 AU $< \Delta \leq 10$ AU (compatible with our L dwarf sample), 11% at 10 AU $< \Delta \leq 100$ AU, and 6% at 100 AU $< \Delta \leq 1000$ AU (Reid & Gizis 1997a). Combining our *HST* observations with the 2MASS limits, we would expect three to four wide ($\Delta > 10$ AU) binaries in the current sample; Martín et al. identified similar expectations in their analysis of the Pleiades sample. The absence of such binaries from both samples implies a 3 σ deficit of wide L dwarf binaries.

4.2. *The Semimajor Axis Distribution of Brown Dwarf Binaries*

Our *HST* observations are aimed at identifying low-mass binary systems. However, both L and T dwarfs are found as companions to higher mass main-sequence stars. We have therefore made a preliminary effort to set the current results in a broader context.

Table 5 collects the available data for binary and multiple systems, which include one or more ultracool dwarf component(s). With the exception of HD 10697B and the Pleiades brown dwarf, PPl 15AB, mass estimates are based on either the detection/nondetection of lithium or the estimated age of the system (usually based on the level of chromospheric activity exhibited by the main-sequence primary star). At present, the selection effects that underlie this sample are too diverse to allow detailed statistical analysis. However, two qualitative comments can be made:

1. Radial velocity surveys, which have identified more than 40 planetary-mass companions of nearby G dwarfs, have discovered a bare handful of brown dwarf companions with orbital semimajor axes $a < 10$ AU. This is the "brown

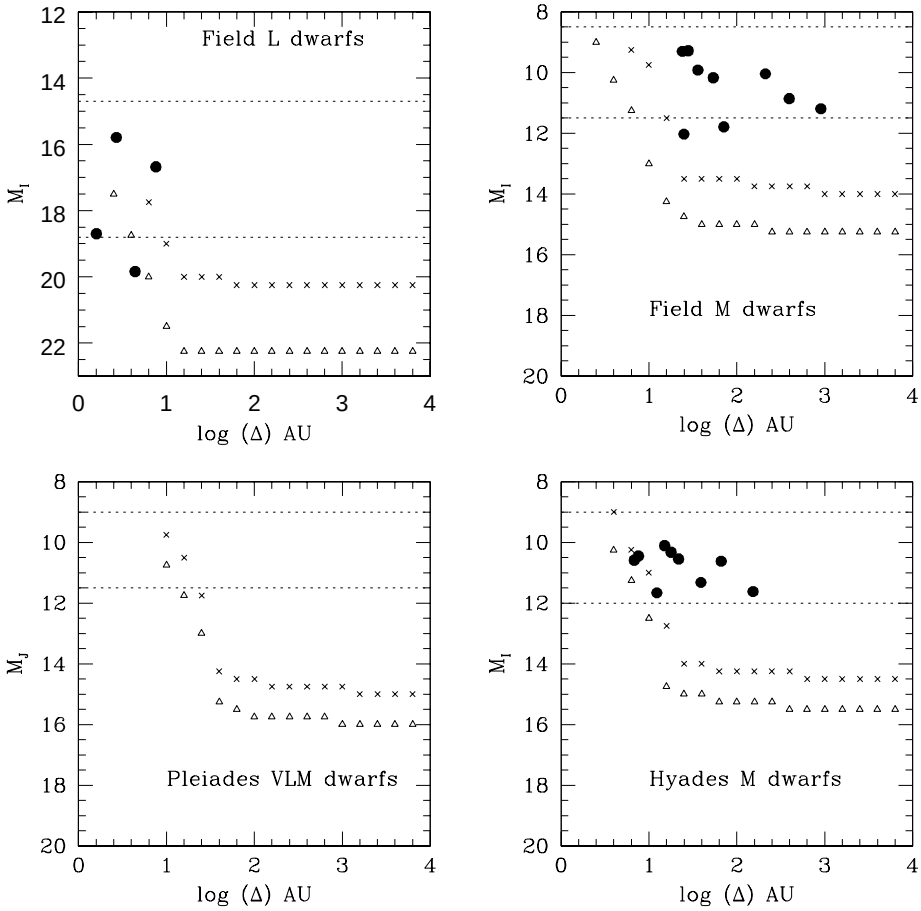

FIG. 13.—Sensitivity limits of four high-resolution imaging surveys for companions. The L dwarf data are from the present paper, the field M dwarfs are from Reid & Gizis (1997a), the Hyades M dwarfs are from Reid & Gizis (1997b), and the Pleiades data are from Martín et al. (2000). Note that we plot M_J for the last mentioned data set. Limiting magnitude (M_I or M_J) is plotted as a function of linear separation from the primary (in AU). Crosses mark the 100% completeness level; open triangles, 50% completeness. The horizontal dotted lines indicate the approximate range of absolute magnitudes of the primaries, and detected companions are plotted as filled circles.

dwarf desert," highlighted by Marcy & Butler (1998). Table 5 shows that brown dwarfs exist as *wide* (10–4000 AU) companions of nearby solar-type stars. Systems with comparable separations but with an M dwarf as the wide component are also known, notably Proxima Cen/α Cen (Matthews & Gilmore 1993).

2. In contrast, all L dwarf/L dwarf binaries detected to date have separations of less than 10 AU, overlapping with the brown dwarf desert in higher mass systems, and most systems have mass ratios near unity. Close brown dwarfs clearly form with greater ease around low-mass primaries (see Basri & Martín 1999).

Figure 14 presents these results in graphical form. The top panel compares the (q, Δ) distribution of the L dwarf binaries listed in Table 5 against similar data for M dwarf binaries within 8 pc of the Sun (from Reid & Gizis 1997a) and for the *HST* M dwarf samples discussed in the previous section. Several features of this diagram demand comment.

First, there is an apparent preference for equal-mass L dwarf/L dwarf binaries. It remains possible that the observed distribution is partly a result of selection effects, since current observations have only limited sensitivity to low-q systems at small Δ (see Fig. 13). Nonetheless, this echoes the bias toward equal-mass systems among M dwarf binaries (Reid & Gizis 1997a, 1997b), where observations extend to lower mass ratios.

Second, no L dwarf/L dwarf binaries are known with separations $\Delta > 10$ AU—is this nature or nurture? There are several possibilities: wide low-mass binaries form, but are stripped by gravitational interactions; wide binaries are inhibited from forming, leading to a truncated semimajor axis distribution and an overall decrease in binary frequency; or formation of wide binaries is inhibited, but close systems form with greater frequency among VLM dwarfs. The last option was suggested by Basri & Martín (1999), prompted by the existence of the short-period Pleiades binary, PPl 15. Better statistics on the frequency of such binaries among VLM dwarfs can constrain the latter two options. We note that Mayor (2000) finds that the fraction of spectroscopic (small separation) binaries is essentially constant at $\sim$12% for nearby stars with spectral types between G and M.

The third outstanding feature of the $[q, \log(\delta)]$ diagram is the prevalence of low-q systems at wide separations. These are low-mass analogues of the wide, common proper motion (CPM) systems made familiar by Luyten's extensive surveys. Such systems are vulnerable to disruption through gravitational encounters with stars and giant molecular clouds, or via tidal effects due to the Galactic field. The

TABLE 5

KNOWN L DWARF/BROWN DWARF BINARIES

System	M_{pri} ($M_\odot$)	M_{sec} ($M_\odot$)	q[a]	Δ AU	References
PPl 15[b]	0.07	0.06	0.86	0.03	1
HD 10697	1.10	0.04	0.035	0.07	2
2M0746	>0.06	>0.06	1.0	2.7	3
2M0920	0.06–0.075	0.06–0.075	0.95	3.2	3
2M0850	<0.06	<0.06	0.75	4.4	3
DENIS 1228	<0.06	<0.06	~1	4.9	4
2M1146	<0.06	<0.06	~1	7.6	5
DENIS 0205	0.06–0.09	0.06–0.09	~1	9.2	5
Gl 229B	0.5	~0.045	~0.1	44	6
TWA 5[b,c]	0.4	0.025	0.06	100	7
GD 165B	>1	<0.08	<0.08	110	8
HR 7329B	~5	<0.05	<0.01	200	9
GJ 1048B	~0.7	<0.08	<0.11	250	10
G196-3B	0.5	~0.025	~0.05	340	11
GJ 1001B	0.4	~0.05	~0.13	180	12
Gl 570D	0.7	~0.05	~0.07	1525	13
Gl 417B	1.0	~0.035	~0.035	2000	14
Gl 584C	1.0	~0.060	~0.060	3600	14

[a] Mass ratios for L dwarf/L dwarf systems are based on the relative K-band luminosity.

[b] Members of Pleiades Cluster or TW Hydrae association.

[c] High-resolution spectroscopy indicates that several other stars in this moving group are binary or multiple systems.

REFERENCES.—(1) Basri & Martín 1999; (2) Zucker & Mazeh 2000; (3) this paper; (4) Martín et al. 1999; (5) Ko99; (6) Nakajima et al. 1995; (7) Lowrance et al. 1999; (8) Becklin & Zuckerman 1988; (9) Lowrance et al. 2000; (10) Gizis, Kirkpatrick, & Wilson 2000; (11) Rebolo et al. 1998; (12) Goldman et al. 1999; (13) Burgasser et al. 2000a; (14) Kirkpatrick et al. 2001.

binding energy of a binary star system is directly proportional to the total mass and inversely proportional to the separation. If we make the reasonable assumption that all binaries are subject to gravitational perturbations of the same average force, then we would expect to find fewer wide binaries with decreasing total system mass. Consequently, low-mass stars and brown dwarfs in wide binaries are more likely to survive if the primary has a relatively high mass, leading naturally to a predominance of low-q systems at large Δ. Indeed, we might expect a characteristic cutoff radius for binary separation as a function of total mass, M_{tot}.

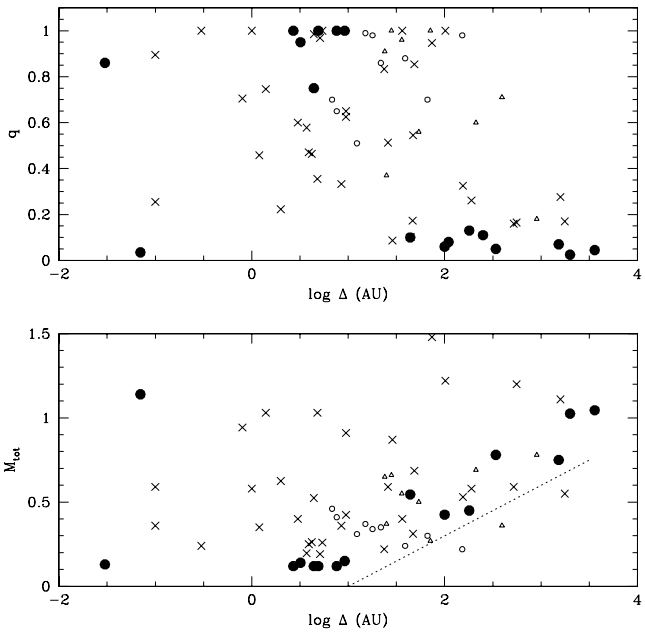

FIG. 14.—The top panel plots the [mass ratio, log(separation)] distribution for L dwarf binaries from Table 5 (*filled circles*) matched against similiar data for M dwarf binaries in the solar neighborhood (*crosses*) and from the HST Hyades (*open circles*) and field (*triangles*) surveys. The lower panel plots the total mass of each binary against log Δ, using the same symbols.

The bottom panel in Figure 14 suggests strongly that there is a correlation between maximum separation and M_{tot}. Such behavior would provide a natural explanation for the decreased *total* binary frequency among M dwarfs (as compared to G dwarfs), while preserving the invariance with mass of the frequency of spectroscopic binaries. However, it is not clear whether this follows the functional form expected for tidal disruption. The dotted line plotted in Figure 14 is

$$\log \Delta_{max} = 3.33 M_{tot} + 1.1 ,$$

i.e., a log-normal relation (the three M dwarf binaries beyond the line are Gl 412AB, RHy 240AB, and MT 3AB). One expects a scaling linearly proportional to M_{tot} for disruption by point source encounters, although circumstances are more complex in the case of an extended potential (Weinberg, Shapiro, & Wasserman 1987). It seems unlikely, however, that the observed rapid decrease in Δ_{max} with M_{tot} is due solely to dynamical evolution.

As a final comment, we note that the wide CPM systems plotted in Figure 14 have dimensions that exceed those of typical protostellar disks. Previous studies have suggested that the relative properties of short- and long-period stellar binaries may differ significantly (Mazeh et al. 1992), perhaps reflecting different formation histories (Mathieu 1994). Individual components in these wide systems may have formed

essentially independently. Indeed, the widest systems may be more akin to residual cluster fragments—that is, progeny of separate cloud cores that retain the motion of the parent cluster. Under this scenario, Gl 584ABC, α Cen/Proxima, Gl 752A/VB10, and their ilk would be minimal examples of Eggen-style moving groups—cousins, rather than siblings.

Further examples of wide L dwarf common proper motion systems will be forthcoming from detailed examination of the photometric catalogs produced by 2MASS, SDSS, and DENIS. The completion of our present survey will provide more detailed information on the prevalence of ultracool dwarf binaries at modest separations.

5. SUMMARY

We have presented high spatial resolution planetary camera observations of 20 L dwarfs. Four are resolved as binary systems with fainter companions at projected separations of 2–8 AU. While our present sample consists of only 20 L dwarfs drawn from a magnitude-limited rather than volume-limited parent sample, the preliminary indications are that the fraction of binary L dwarfs at separations exceeding 10 AU is *lower* than the empirical value of $\sim$20% measured for M dwarf systems. Both L and T dwarfs, however, are found as wide CPM companions of higher mass, main-sequence stars.

Three of the four binaries in our current L dwarf sample have components with similar luminosities, implying nearly equal masses; 2M0850AB, however, has a secondary component that is 1.3 mag fainter than the primary. The primary has strong lithium absorption, indicating a mass below 0.06 $M_{\odot}$, and comparison with theoretical models calculated by Burrows et al. (1993, 1997) suggests a secondary/primary mass ratio of $\sim$0.8. 2M0850B has $M_I = 19.8 \pm 0.25$ and is likely to be either a very late type L dwarf ($\sim$L9) or an early-type T dwarf.

Unequal-mass brown dwarf binaries offer an effective means of constraining theoretical models. Since the components are coeval, both must lie on the same isochrone in the ($\log L$, $\log T_{\rm eff}$) plane. This technique has been used to test models of pre–main-sequence stars and brown dwarfs against observations of young, multiple systems (see, e.g., White et al.'s (1999) analysis of data for GG Tau). Once accurate effective temperatures are available for L dwarf systems, similar methods can be used to probe parameter space at lower masses and temperatures, as illustrated in Figure 10. In particular, this approach offers excellent promise for resolving questions concerning the L/T transition phase: determining both the critical threshold temperature for the onset of the change from CO-dominated spectra (L dwarfs) to CH_4 spectra (T dwarfs), and the rapidity of the transformation. More detailed observations of these, and other, binary L dwarf systems will provide benchmarks for future theoretical models of low-mass stars and brown dwarfs.

The authors would like to thank the referee, Gibor Basri, for useful criticism. This work is based on observations with the NASA/ESA *Hubble Space Telescope* obtained at the Space Telescope Science Institute, which is operated by the Association of Universities for Research in Astronomy, Inc., under NASA contract NAS 5-26555. Our research was supported by NASA through STScI grant GO-08146.01-97A.

REFERENCES

Basri, G., & Martín, E. L. 1999, AJ, 118, 2460
Basri, G., Mohanty, S., Allard, F., Hauschildt, P. H., Delfosse, X., Martín, E. L., Forveille, T., & Goldman, B. 2000, ApJ, 538, 343
Becklin, E. E., & Zuckerman, B. 1988, Nature, 336, 656
Bessell, M. S. 1991, A&AS, 83, 357
Branch, D. 1976, ApJ, 210, 392
Burgasser, A. B., et al. 2000a, ApJ, 531, L57
Burgasser, A. J., Kirkpatrick, J. D., Reid, I. N., Liebert, J., Gizis, J. E., & Brown, M. E. 2000b, AJ, 120, 473
Burrows, A., Hubbard, W. B., Saumon, D., & Lunine, J. I. 1993, ApJ, 406, 158
Burrows, A., et al. 1997, ApJ, 491, 856
Burrows, A., & Sharp, C. M. 1999, ApJ, 512, 843
Chabrier, G., Baraffe, I., Allard, F., & Hauschildt, P. 2000, ApJ, 542, 464
Dahn, C. C., et al. 1999, in ASP Conf. Ser. 213, From Giant Planets to Cool Stars, ed. C. Griffiths & M. Marley (San Francisco: ASP), 74
Dahn, C. C., et al. 2001, in preparation
Delfosse, X., et al. 1997, A&A, 327, L25
Duquennoy, A., & Mayor, M. 1991, A&A, 248, 485
Fan, X., et al. 2000, AJ, 119, 928
Fegley, B., & Lodders, K. 1996, ApJ, 472, L37
Fischer, D. A., & Marcy, G. W. 1992, ApJ, 396, 178
Geballe, T., Kulkarni, S. R., Woodward, C. E., & Sloan, G. C. 1996, ApJ, 467, L101
Gizis, J. E., Kirkpatrick, J. D., & Wilson, J. C. 2001, AJ, submitted
Goldman, B., et al. 1999, A&A, 351, L5
Golimowski, D. A., Burrows, C. J., Kulkarni, S. R., Oppenheimer, B. R., & Brukardt, R. A. 1998, AJ, 115, 2579
Holtzman, J. A., Burrows, C. J., Casertano, S., Hester, J. J., Trauger, J. T., Watson, A. M., & Worthey, G. 1995, PASP, 107, 1065
Jones, H. R. A., Longmore, A. J., Jameson, R. F., & Mountain, C. M. 1994, MNRAS, 267, 413
Kirkpatrick, J. D., Allard, F., Bida, T., Zuckerman, B., Becklin, E. E., Chabrier, G., & Baraffe, I. 1999a, ApJ, 519, 834
Kirkpatrick, J. D., et al. 1999b, ApJ, 519, 802 (K99)
———. 2000a, AJ, 120, 447 (K00)
———. 2001, in preparation
Koerner, D., Kirkpatrick, J. D., McElwain, M. W., & Bonaventura, N. R. 1999, ApJ, 526, L25
Leggett, S. K., et al. 2000, ApJ, 536, L35
Leggett, S. K., Toomey, D. W., Geballe, T. R., & Brown, R. H. 1999, ApJ, 517, L139
Lodders, K. 1999, ApJ, 519, 793
Lowrance, P. J., et al. 1999, ApJ, 512, L69
———. 2000, ApJ, 541, 390
Marcy, G. W., & Butler, P. 1998, ARA&A, 36, 57
Marley, M. S., Saumon, D., Guillot, T., Freedman, R. S., Hubbard, W. B., Burrows, A., & Luminine, J. I. 1996, Science, 272, 1919
Martín, E. L., Brandner, W., & Basri, G. 1999, Science, 283, 1718
Martín, E. L., Brandner, W., Bouvier, J., Luhman, K. L., Stauffer, J., Basri, G., & Zapatero Osorio, M. R. 2000, ApJ, 543, 299
Mathieu, R. D. 1994, ARA&A, 32, 465
Matthews, K., Nakajima, T., Kulkarni, S. R., & Oppenheimer, B. R. 1996, AJ, 112, 1678
Matthews, R., & Gilmore, G. 1993, MNRAS, 261, L5
Mayor, M. 2000, in ASP Conf. Ser., Microlensing 2000, ed. J. W. Menzies & P. D. Sackett (San Francisco: ASP), in press
Mazeh, T., Goldberg, D., Duquennoy, A., & Mayor, M. 1992, ApJ, 401, 265
Nakajima, T., Oppenheimer, B. R., Kulkarni, S. R., Golimowski, D. A., Matthews, K., & Durrance, S. T. 1995, Nature, 378, 463
Noll, K. S., Geballe, T. R., Leggett, S. K., & Marley, M. S. 2000, ApJ, 541, L75
Öpik, E. 1924, Publ. Obs. Astron. Univ. Tartu, 25, 6
Rebolo, R., Martín, E. L., & Magazzu, A. 1992, ApJ, 389, L83
Rebolo, R., Zapatero Osorio, M. R., Madruga, S., Bejar, V. J. S., Arribas, S., & Licandro, J. 1998, Science, 282, 1309
Reid, I. N., & Gizis, J. E. 1997a, AJ, 113, 2246
———. 1997b, AJ, 114, 1992
Reid, I. N., et al. 1999, ApJ, 521, 613
———. 2001, AJ, submitted
Reid, I. N., Kirkpatrick, J. D., Williams, R., Liebert, J., & Burgasser, A. 2000, AJ, 119, 369
Ruiz, M. T., Leggett, S. K., & Allard, F. 1997, ApJ, 491, L107
Tinney, C. G., Reid, I. N., & Mould, J. R. 1993, AJ, 105, 1045
Tsuji, T. 1964, Ann. Tokyo Astron. Obs., 9, 1
Weinberg, M. D., Shapiro, S. L., & Wasserman, I. 1987, ApJ, 312, 367
White, R. J., Ghez, A. M., Reid, I. N., & Schultz, G. 1999, ApJ, 520, 811
Zucker, S., & Mazeh, T. 2000, ApJ, 531, L67